Journal of the European Ceramic Society **14** (1994) 343–349

Pressureless Sintering and Phase Relationship of Samarium α-Sialons

Yi-Bing Cheng

Department of Materials Engineering, Monash University, Melbourne, Victoria 3168, Australia

&

Derek P. Thompson

Department of Mechanical, Materials and Manufacturing Engineering, University of Newcastle upon Tyne, UK

(Received 23 February 1994; accepted 31 March 1994)

Abstract

The sinterability of samarium α-sialon (α') compositions and the phase assemblage around the α-sialon region have been studied. Samarium oxide is an effective stabiliser for α-sialons and has a significantly superior densification effect on α-sialon ceramics than neodymium and yttrium oxides. The 21R polytypoid phase is found to be in equilibrium with Sm α-sialons instead of 12H as found in the yttrium system. Two phase regions containing the α-sialon phase have been found, namely, α'–β'–21R–L (liquid) and α'-21R-27R-L. Compositions in the α'–β'–21R–L region possess relatively more liquid phase than those in other α-sialon-containing phase regions. With careful compositional selection, almost fully dense α-sialon ceramics can be prepared by pressureless sintering.

Die Sinterfähigkeit von Samarium α-Sialon (α') Verbindungen und die verschiedenen zum α-Sialon-Gebiet benachbarten Phasen wurden untersucht. Samariumoxid ist ein effektives Stabilisierungsmittel für α-Sialone und besitzt einen weit besseren Verdichtungseffekt auf α-Sialonkeramiken als Neodym- und Yttriumoxid. Die Untersuchungen ergaben, daß die 21R polytypoide Phase im Gleichgewicht mit Sm α-Sialonen ist im Gegensatz zu 12H im Yttriumsystem. Zwei Phasengebiete, die α-Sialone enthalten, konnten nachgewiesen werden, nämlich α'–β'–21R–L (flüssig) und α'–21R–27R–L. Verbindungen im α'–β'–21R–L Gebiet besitzen mehr flüssige Phase als Verbindungen in anderen Gebieten die α-Sialon enthalten. Bei sorgfältiger Auswahl der Zusammensetzung kann beinahe vollständige Dichte beim drucklosen Sintern der α-Sialone erzielt werden.

On a étudié la frittabilité de sialons α de samarium (α'), ainsi que les phases présentes dans le domaine d'existence du sialon α. L'oxyde de samarium est un stabilisateur efficace pour les sialons α et a un effet plus important sur la densification des céramiques à base de sialon α que l'oxyde de néodymium ou l'oxyde d'yttrium. On a trouvé que c'est le polytype 21R qui est en équilibre avec le sialon α–Sm au lieu du polytype 12H dans le système yttrié. On a trouvé deux domaines d'existence du sialon α, α'–β'–21R–L (liquide) et α'–21R–27R–L. Les compositions dans le domaine α'–β'–21R–L contiennent relativement plus de phase liquide que ceux de autres domaines contenant du sialon α. Si l'on choisit soigneusement la composition, on peut préparer des céramiques de sialon α pratiquement denses à 100%, par frittage naturel.

1 Introduction

It is essential to add sintering additives in the densification of silicon nitride based materials because strong covalent bonds inhibit diffusion at sintering temperatures. The added oxides react with the surface silica on the silicon nitride powder together with a little silicon nitride giving an oxynitride liquid which helps the transformation from α to β silicon nitride and facilitates densification of the materials. The introduction of alumina into the system makes the liquid-phase sintering process occur more readily and results in the formation of sialons.[1] However vitreous or crystalline secondary phases will be produced after cooling, which impair high-temperature mechanical properties, such as strength and creep resistance.

Journal of the European Ceramic Society 0955-2219/94/$7.00

α-sialon (α'), unlike β-sialon (β'), can accommodate additional cations (e.g. densification additives) into its structure. The general formula for α-sialon solid solutions can be expressed as $R_xSi_{12-(m+n)}Al_{m+n}O_nN_{16-n}$, where R is a large cation (typically Li, Mg, Ca, Y and Ln with $Z \geq 60$) and $0 < x \leq 2$. α-Sialons offer promising advantages over β-sialon materials, namely, increased hardness and the possibility of producing a single-phase sialon ceramic with a minimum of grain boundary phases.[2,3] However, because of the high nitrogen concentration and the requirement for an appropriate cation as a stabiliser, there is a much more limited choice of additives that are suitable for the preparation of dense α-sialon ceramics.

A successful oxide additive (RO_x) for α-sialon ceramics should meet a number of criteria: (a) the cation R must have an appropriate size to be accommodated into the α-sialon structure; (b) the eutectic temperature of the oxide-containing liquid should be lower than the α-sialon formation temperature but high enough to give good creep behaviour; (c) no intermediate phase produced by the additive during sintering should prevent densification; (d) it is desirable to have a large liquid phase region in the R–Si–Al–O–N system in equilibrium with the α-sialon phase. Although a number of cations can stabilise α-sialon structures, extensive studies have been carried out mainly in the yttrium-containing system.[3] However, recent investigations in rare earth sialon systems have found that the sintering behaviour of α-sialon ceramics varies significantly when different lanthanide oxides are used, and some of the results suggested the possibility of densifying α-sialon ceramics by pressureless sintering.[4–7] A better understanding of phase equilibria at various temperatures is imperative for the preparation of α-sialon materials because it has been found that the appearance of undesirable intermediate phases (e.g. melilite) in some systems could hinder densification and reduce the yield of the α-sialon phase.[5,6]

In this paper the results of pressureless sintering of Sm-containing α-sialon ceramics are reported and phase relationships in the regions associated with the α-sialon phase discussed.

2 Experimental

About 50 g of a mixture containing Si_3N_4 (Starck Berlin, LC10), AlN (Starck Berlin, Grade B), Al_2O_3 (Alcoa, A17) and Sm_2O_3 (RE Acton, Rare Earth Products, 99·9%) were mixed with Si_3N_4 balls for three days. Cold isostatic pressing was used for the green body formation. Pellets packed with an Si_3N_4/BN powder mixture were placed in a graphite crucible and sintered in a carbon resistance furnace which had a fast natural cooling rate of 50°C min^{-1} from 1800 to 1200°C. Heat treatment was carried out in an alumina tube furnace in flowing nitrogen.

A Hägg–Guinier focusing camera was used for crystalline phase characterisation and a Camscan S4-80DV microscope for SEM observation. Bulk densities of sintered samples, after boiling in water for 1 h, were measured using water immersion.

3 Results and discussion

3.1 Sintering of Sm α-sialon materials

A series of samarium-containing sialon compositions were designed to investigate the sinterability of the samples and the resulting phase assemblages around the α-sialon region. Table 1 shows percentages of the starting ingredients in the samples and the actual formulae after taking account of 1·98 and 2 wt% of oxygen on the surfaces of Si_3N_4 and AlN powders respectively. The α-sialon phase region is located within the Si_3N_4–4/3(AlN .

Table 1. Starting compositions (wt%) and actual formulae for Sm α-sialon materials

Sample	*Si_3N_4*	*AlN*	*Al_2O_3*	*Sm_2O_3*	*SiO_2*	*Actual formula*	*k*
SA2	69·14	20·86	0	10·00	—	$Sm_{0.348}Si_{9.011}Al_{3.102}O_{1.245}N_{14.642}$	0·762
SA3	66·62	18·59	1·50	13·29	—	$Sm_{0.481}Si_{8.954}Al_{3.031}O_{1.702}N_{14.313}$	0·748
SA4	67·62	19·09	2·00	11·29	—	$Sm_{0.404}Si_{8.919}Al_{3.112}O_{1.671}N_{14.298}$	0·753
SA5	68·71	16·00	2·00	13·29	—	$Sm_{0.481}Si_{9.226}Al_{2.694}O_{1.790}N_{14.291}$	0·741
SA6	61·62	15·75	3·61	19·44	—	$Sm_{0.759}Si_{8.891}Al_{2.872}O_{2.230}N_{14.007}$	0·724
SA7	62·02	16·28	9·43	12·27	—	$Sm_{0.439}Si_{8.264}Al_{3.633}O_{3.037}N_{13.065}$	0·739
SA8	72·50	14·27	2·00	11·23	—	$Sm_{0.379}Si_{9.548}Al_{2.381}O_{1.668}N_{14.403}$	0·742
SA8·5	70·03	15·84	0	11·23	2·90	$Sm_{0.398}Si_{9.513}Al_{2.385}O_{1.903}N_{14.199}$	0·739
SA9	68·14	12·84	3·67	13·30	2·05	$Sm_{0.480}Si_{9.361}Al_{2.421}O_{2.503}N_{13.716}$	0·725
SA10	75·87	11·89	1·00	11·24	—	$Sm_{0.397}Si_{9.982}Al_{1.908}O_{1.493}N_{14.617}$	0·738
SA20	72·50	16·00	0	11·50	—	$Sm_{0.398}Si_{9.570}Al_{2.414}O_{1.334}N_{14.682}$	0·748
SA30	75·87	11·89	1·00	11·24	1·5 C	$Sm_{0.397}Si_{9.982}Al_{1.908}O_{1.493}N_{14.617}$	0·738[a]

[a] Without considering the carbon black added in the sample.

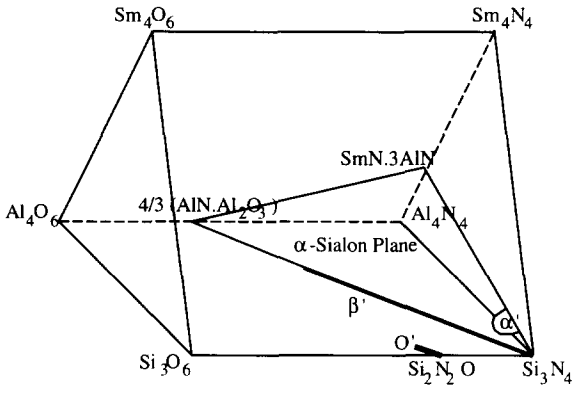

Fig. 1. Position of α-sialon plane in the Sm–Si–Al–O–N sialon system.

Al_2O_3)–SmN . 3AlN plane (Fig. 1). If the samarium content is discounted, any composition on the α-sialon plane should have a ratio, k, of (Si, Al) : (O, N) equal to 3 : 4. Therefore, if a designed composition is just on the plane, its k value is 0·75, otherwise it can be either above the plane if $k <$ 0·75 or below the plane if $k >$ 0·75. It is seen that most of the compositions listed in Table 1 are slightly above the plane.

The samples were pressureless sintered at various conditions and their densities and X-ray results are presented in Table 2. Samarium is an effective stabiliser for the α-sialon phase and materials containing more than 90% α-sialon can be prepared with a proper selection of compositions (Fig. 2). The displacement of these compositions from the exact α-sialon plane results in three crystalline phases being commonly found in most of these samples, namely, α-sialon, β-sialon and the sialon polytypoids. In an R–Si–Al–O–N sialon system, there should be four phases for an ultimate equilibrium state; the failure to identify the fourth one from XRD results is due to the amorphous nature of the grain boundary phase formed on fast cooling. In comparison, one sample (SA4) was cooled slowly at less than 30°C min^{-1} from 1800°C, and wollastonite was found as an additional crystalline phase, which was a devitrification product of the glassy phase commonly observed in sialon materials on slow cooling.[8]

Significant densification was achieved in most of the Sm α-sialon samples when the sintering temperature was higher than 1750°C and the characteristics of liquid-phase sintering were apparent in the final microstructures of the materials (Fig. 3). Although the difficulties of producing dense α-sialon ceramics are commonly known in a number of sialon systems, the present results suggest that in the samarium-containing system, α-sialon ceramics could be densified by pressureless sintering. It is evident that the density increases if the composition is above the α-sialon plane (i.e. $k <$ 0·75) due to the presence of a liquid phase, otherwise the density is generally low, due to insufficient liquid if the composition is below or just on the plane.

The involvement of an adequate amount of low viscosity liquid during sintering is most important to the densification process and this is best illustrated by the difference in densification behaviour between samples SA10 and SA30. Both SA10 and SA30 have the same basic compositions and the only difference is 1·5 wt% additional carbon added in sample SA30 (Table 1). The carbon black in SA30 reacts with the oxides on the surfaces of Si_3N_4 and AlN powders and significantly reduces the oxygen content in the system. As a result, the k value can be increased from the designed $k <$ 0·75 in SA10 to $k \geq$ 0·75 in SA30 (Table 1), shifting the composition close to or even under the α-sialon plane. This would lead to a reduction in the amount of liquid phase and an increase in its

Table 2. Density and X-ray results of samples sintered under different conditions

Sample	*Temperature (°C)/ time (h)*	*D (g cm^{-3})*	*α'*	*β'*	*21R*	*12H*	*M'_{ss}*	*$2H^{\delta}$*
SA2	1800/2	2·985	vs[a]					
	1600/1, 1750/2	2·644	vs		w			
SA3	1800/2	—	vs		w		w	
	1600/1, 1750/2	3·326	vs	vvw	w		vw	
SA4	1800/2	3·327	vs	vw	mw			
	1600/1, 1750/2	3·279	vs	vw	mw			
SA5	1800/1	3·336	vs	vw	w		w	
SA6	1800/1	3·570	s	w	w		ms	
SA7	1800/1	3·409	m	s		m		
SA8	1500/0·5, 1800/2	3·369	vs	w	w			
	1800/2	3·299	s	w	w			
SA8·5	1800/2	3·373	s	m	vw			
SA9	1500/0·5, 1800/2	3·418	ms	m	w			
SA10	1800/2	3·345	ms	m	vvw			
SA20	1500/0·5, 1780/1·5	2·869	vs	vvw	vvw			
SA30	1500/0·5, 1780/1·5	2·783	vs					vw

[a] X-Ray intensities: s, strong; m, medium; w, weak; v, very.

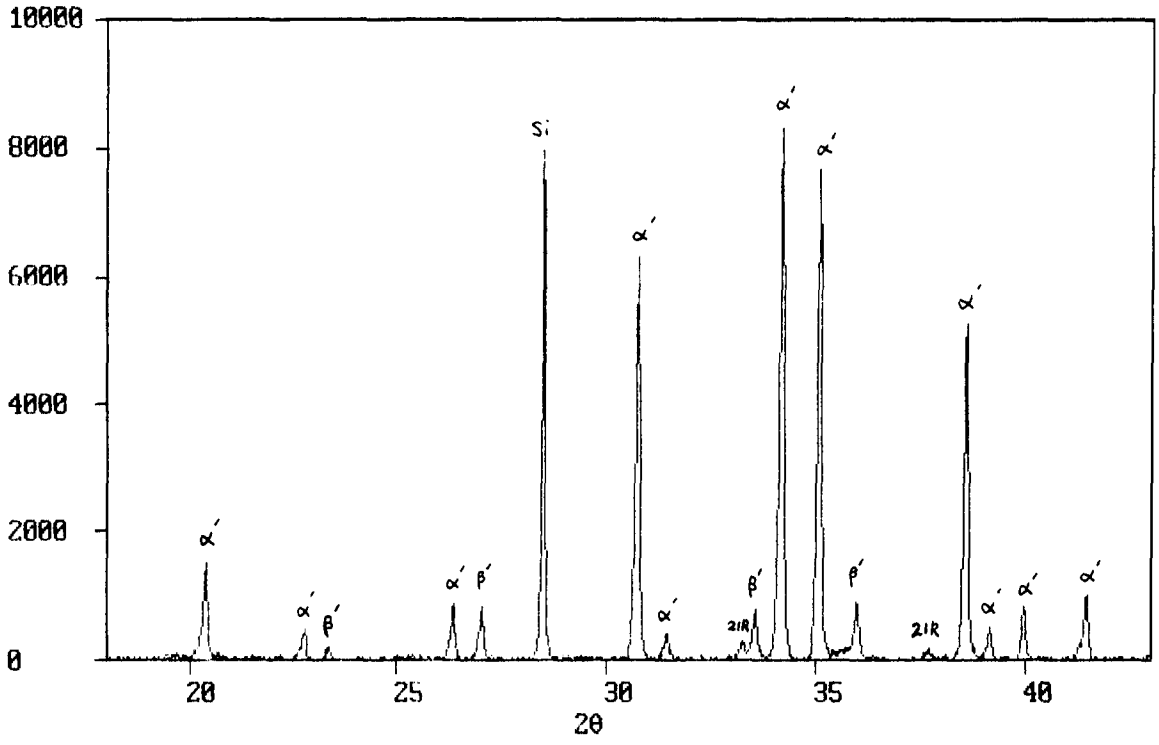

Fig. 2. XRD result of SA8 sample after sintering at 1800°C, where α': α-sialon; β': β-sialon; 21R: 21R polytypoid phase. Silicon was used as a calibration standard.

viscosity. After sintering, it is seen that the density of sample SA30 has been considerably lowered and the crystalline phases detected from XRD are accordingly changed from α'–β'–21R in SA10 to α'–$2H^{\delta}$ in SA30 (Table 2). The α'-$2H^{\delta}$-L phase region was not found in the yttrium α-sialon system[9] and it suggests that the additional carbon may have shifted the SA30 composition under the α-sialon plane where no liquid phase exists and $2H^{\delta}$ is more likely to form.

The present results indicate that there is a tie line between the liquid phase and α-sialon regions in the Sm–Si–Al–O–N system although this tie line has not crossed the α-sialon plane, offering a promise of densifying α-sialon materials in the system by pressureless sintering. This result is different from that observed in the Nd sialon system in which the α'-liquid tie line was interrupted by a melilite phase which was persistent even at 1800°C.[7,10] It is believed that the persistence of the melilite phase in the Nd α-sialon system at sintering temperatures reduces the amount of liquid phase in the sample and severely undermines the precipitation and densification of α-sialon materials. Melilite was also found as an intermediate phase during the sintering of Sm α-sialon ceramics and it formed as a solid solution with aluminium, referred to as M'_{ss}.[12] In the present experiment, however, the Sm M'_{ss} phase disappeared from most of the samples when sintered at 1800°C (Table 2). The better densification behaviour in the Sm α-sialon system is attributed to a relatively low melting point of the M'_{ss} phase at sintering temperatures, releasing large amounts of liquid for densification.

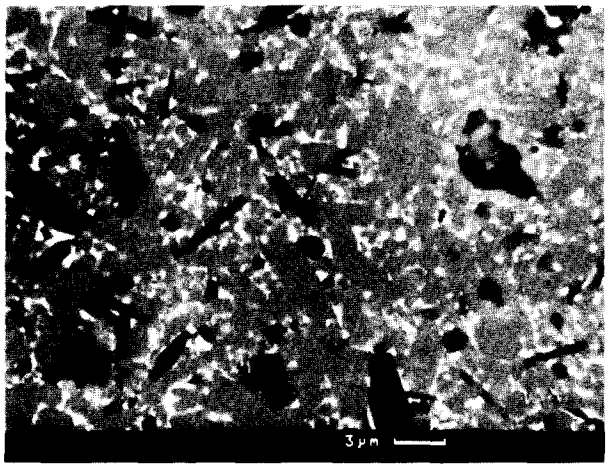

Fig. 3. SEM microstructure of SA8 sample pressureless sintered at 1800°C. The dark grey phases are β-sialon and 21R, the light grey is α-sialon and the white phase is grain boundary glass.

Although the k value can be used to estimate the position of a composition relative to the α-sialon plane, it is certainly not a rigid criterion, particularly when the k value is close to 0·75, due to the erratic amount of surface oxides in the non-oxide powders. Moreover, a liquid phase appearing in the compositions above the α-sialon plane may not guarantee full densification because the final density of the materials depends critically on the amount and viscosity of the liquid. Sample SA4 had a designed k value of 0·753 (i.e. just below the α-sialon plane) but showed a reasonable density of 3·327 g cm^{-3} at 1800°C. In contrast, the poor density of sample SA20 indicated that the

Table 3. Lattice parameters of sialon phases in different samples

Sample	*α'*			*β'*		
	a(Å)	*c*(Å)	*c/a*	*a*(Å)	*c*(Å)	*z*
SA2	7·814	5·691	0·728			
SA3	7·810	5·690	0·729	7·621	2·918	0·53
SA4	7·816	5·698	0·729			
SA5	7·811	5·690	0·728	7·621	2·919	0·55
SA7	7·809	5·688	0·728	7·630	2·925	0·81
SA8	7·814	5·692	0·728	7·622	2·921	0·61
SA8·5	7·816	5·688	0·728	7·630	2·923	0·78
SA9	7·807	5·687	0·728	7·620	2·921	0·58
SA10	7·810	5·688	0·728	7·622	2·921	0·63
SA20	7·821	5·699	0·729			
SA30	7·819	5·695	0·728			

liquid phase was not effective in densification although its k value was 0·748, i.e. above the α-sialon plane. Phase transformation between Si_3N_4 and α/β-sialon phases has been complete in sample SA20. According to the dissolution–precipitation sintering mechanism, there must be a transient liquid in this sample at some stage of sintering, from which the sialon phases have precipitated. However, it is clear that this transient liquid alone, which is very viscous due to high nitrogen content, has not provided sufficient viscous flow to enable complete densification. It is therefore suggested that a large amount of low viscosity liquid phase present during the precipitation of the sialon phases is important for densification.

3.2 Phase relationships involving Sm α-sialon phases

The cell dimensions of α- and β-sialon phases in selected samples are given in Table 3. As predicted, the variation in cell parameters for α-sialons is relatively small, although the starting compositions are widely spread on the plane; these data are generally in good agreement with the measurements described in Ref. 13. The maximum z-value of β-sialon phases compatible with Sm α-sialon is about 0·8 (Table 3). Compared with the yttrium system, this value is similar to the results reported by some researchers (z = 0·6),[14] but considerably lower than that given by others (z = 1·2) for unknown reasons.[9] The cell dimensions of Sm α-sialon phases are in the range a: 7·810–7·820 (Å), c: 5·685–5·695 (Å). A homogeneous lattice expansion with a constant c/a ratio of 0·728–0·729 indicates a random substitutional replacement of the Si–N bond by both Al–O and Al–N bonds in α-sialon structures. In comparison to the data recently given by Sun *et al.*,[15] the α-sialon phase in Table 3 corresponds to a terminal composition $R_{0.4}Si_{9.2}Al_{2.8}O_{1.6}N_{14.4}$, i.e. m = 1·2 and n = 1·6 in the formula. The much smaller size of Y^{3+} (r = 0·893 Å) and Sm^{3+} (r = 0·964 Å) ions, compared to the mean size of the interstitial voids in the α-sialon structure (d = 2·59 Å)[16] makes this comparison valid.

Phase relationships in the samarium α-sialon plane are different from those in the yttrium system. In the yttrium sialon system, 12H was more commonly found when the z value of the β-sialon phase was high (z = 1·2).[9] In the Sm system, however, instead of having an α'–β'–12H–L phase region, the noticeable difference is that there is a much larger α'–β'–21R–L four phase region. The 21R sialon polytypoid phase was more stable in equilibrium with Sm α-sialon phases when the z value of the β-sialon phase was below 0·8; above this value 12H was found. It is reasonable to assume that the stability of the polytypoid phase varies according to the aluminium content of the sialon phases. Figure 4 shows the observed phase relationships around the α-sialon region at 1800°C. It is seen that all the X-ray results in Table 2 fit the diagram very well apart from those for SA7. It is not clear at the moment why a small amount of α-sialon has been observed in SA7 in which there should be only β-sialon and 12H phases according to the depicted phase diagram.

Correct selection of starting composition is imperative for good sinterability of α-sialon materials. There are two phase regions in which a liquid phase may be involved during the sintering of

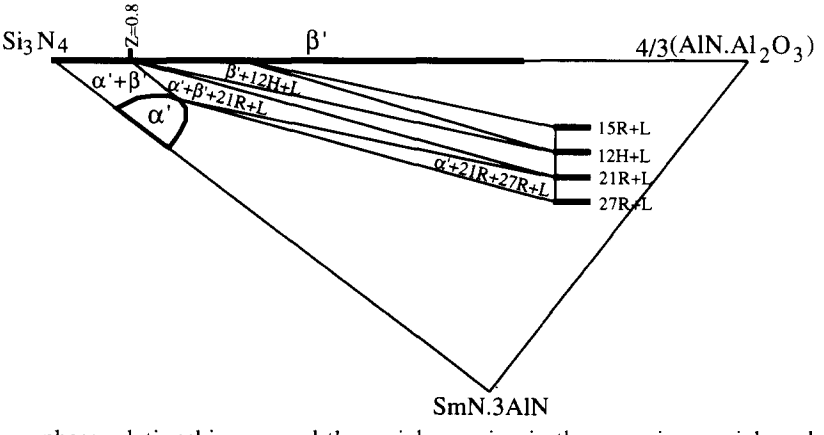

Fig. 4. Behaviour phase relationships around the α-sialon region in the samarium α-sialon plane at 1800°C.

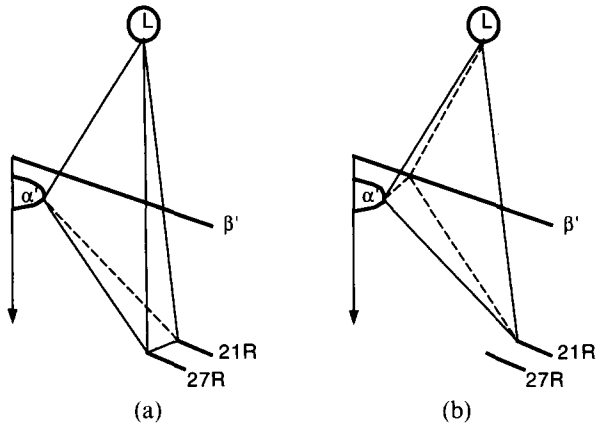

Fig. 5. Two-phase regions involving α-sialon phases at 1800°C; (a) α'–21R–27R–L and (b) α'–β'–21R–L.

α-sialons, namely α'–21R–27R–L and α'–β'–21R–L respectively (Fig. 5). Compositions SA2 and SA3 are in the α'–21R–27R–L phase region and the rest of the samples are in the α'–β'–21R–L tetrahedron. Failure to identify 27R in SA2 was due to the scarcity of the phase and the strong overlapping of the XRD profiles of 21R and 27R. Composition SA4 was also in the α'–21R–27R–L region and other studies have found no β-sialon phase in this sample.[7] The phase compatibility regions in this part of the phase diagram are all very narrow because of the similarity in compositions of the polytypoid phases. Slight compositional variation could significantly change the ratio of α: β sialon and the amount of liquid phase, and/or shift the sample from one phase region to another, resulting in considerable change in the densification behaviour of the samples. This is mainly due to the fact that the amount of liquid phase in equilibrium with β-sialon is relatively larger than that with α-sialon compositions. The β-sialon phase is not- compatible with melilite, whereas the α-sialon is.[17] The liquid phase in equilibrium with β-sialon would assist in the dissolution of melilite and hence improve densification. An important observation is that although only about 10% β-sialon has been introduced into the SA8 composition, the material can be densified to 99% of the hot pressed density by pressureless sintering.[7] It is believed that this principle is of general application so that as more β-sialon is added to α-sialon materials a composite with better densification and improved mechanical properties is obtained. So it is concluded that for best results, materials should be selected within the α'-β'-21R-L phase tetrahedron.

It should be pointed out that the liquid phase denoted in the phase tetrahedra of Fig. 5 is the residual liquid after the precipitation of α/β-sialons. This liquid is in equilibrium with the solid sialon phases at a particular temperature, and its composition and properties obviously vary with temperature. The amount and viscosity of this liquid at the sintering temperature determines the sintering behaviour and hence a better understanding of this liquid at sintering temperatures remains an important topic for future studies.

4 Conclusion

Samarium α-sialon ceramics show different phase relationships and densification characteristics compared with equivalent yttrium and neodymium sialon materials. The type of polytypoid phase compatible with the sialon phases varies with the aluminium content of β-sialon, and the 21R polytypoid phase is commonly observed in Sm α–β–sialon ceramics. There is a tie line between the liquid and the α-sialon phase region and this is not interrupted by any other phases at 1800°C. However, the liquid phase does not extend beyond the nitrogen-rich side of the α-sialon plane. Sm-containing sialon liquid has a relatively low viscosity. For compositions above the α-sialon plane, therefore, samarium oxide shows superior densification on pressureless sintering. There are two phase regions, α'–21R–27R–L and α'–β'–21R–L, in which the α-sialon phase is compatible with liquid phase. However, a small amount of additional β-sialon in α-sialon ceramics significantly improves the densification behaviour of these materials.

Acknowledgment

The financial support by Cookson Group plc, UK, during the period when the work was carried out is sincerely appreciated.

References

1. Jack, K. H., Review, Sialons and related nitrogen ceramics. *J. Mat. Sci.*, **11** (1976) 1135–58.
2. Ekström, T. & Nygren, M., Sialon ceramics. *J. Am. Ceram. Soc.*, **75** (1992) 259–76.
3. Cao, G. Z. & Metselaar, R., α'-Sialon ceramics: A review. *Chem. Mat.*, **3** (1991) 242–3.
4. Ekström, T., Sialon ceramics sintered with yttria and rare earth oxides. In *MRS Symposium Proceedings: Silicon Nitride Ceramics—Science and Technological Advances*, Vol. 287, ed. I-Wei Chen *et al.* MRS, 1993, pp. 121–32.
5. Wang, P. L., Sun, W. Y. & Yen, T. S., Formation and densification of *R*-α'-sialons (*R* = Nd, Sm, Gd, Dy, Er and Yb). In *MRS Symposium Proceedings: Silicon Nitride Ceramics–Science and Technological Advances*, Vol. 287, ed. I-Wei Cheng *et al.* MRS, 1993, pp. 387–92.
6. O'Reilly, K. P. J., Redington, M., Hampshire, S. & Leigh, M., Parameters affecting pressureless sintering of α'-sialons with lanthanide modifying cations. In *MRS Symposium Proceedings: Silicon Nitride Ceramics–Science and Technological Advances*, Vol. 287, ed. I-Wei Cheng *et al.* MRS, 1993, pp. 393–8.

7. Cheng, Y.-B. & Thompson, D. P., Preparation and grain boundary heat-treatment of samarium α-sialon ceramics. *J. Eur. Ceram. Soc.*, **14** (1994) 13–21.
8. Korgul, P. & Thompson, D. P., Crystallisation behaviour of N-α-wollastonite glasses. In *Complex Microstructures, Brit. Ceram. Proc.*, No. 42, ed. R. Stevens & D. Taylor. 1989, pp. 69–80.
9. Slasor, S. & Thompson, D. P., Preparation and characterisation of α'-sialons. In *Non Oxide Technical and Engineering Ceramics*, ed. S. Hampshire. Elsevier Applied Science, London, 1986, pp. 223–30.
10. Slasor, S., Liddell, K. & Thompson, D. P., The role of Nd_2O_3 as an additive in the formation of α' and β' sialons. In *Special Ceramics 8*, ed S. P. Howlett & D. Taylor. The Institute of Ceramics, 1986, pp. 51–64.
11. Sun, W. Y., Wu, F. Y. & Yen, T. S., Studies of the formation of α' and α'-β' sialon. *Mater. Lett.*, **6** (1987) 11–15.
12. Cheng, Y.-B. & Thompson, D. P., Aluminium-containing nitrogen melilite phases. *J. Am. Ceram. Soc.*, **77** (1994) 143–8.
13. Huang, Z.-K., Tien, T.-Y. & Yen, T.-S., Subsolidus phase relationships in Si_3N_4–AlN–rare-earth oxide systems. *J. Am. Ceram. Soc.*, **69** (1986) C241–2.
14. Ukyo, Y. & Wada, S., α'/β' sialon composites. In *Grain Boundary Controlled Properties of Fine Ceramics*, ed. K. Ishizaki *et al.* Elsevier Applied Science, London, 1992, pp. 112–24.
15. Sun, W. Y., Tien, T. Y. & Yen, T. S., Solubility limits of α'-sialon solid solutions in the system Si, Al, Y/N, O. *J. Am. Ceram. Soc.*, **74** (1991) 2547–50.
16. Izumi, F., Mitomo, M. & Suzuki, J., Structure refinement of yttrium α-sialon from X-ray powder profile data. *J. Mat. Sci. Lett.*, **1** (1982) 533–5.
17. Sun, W. Y., Yan, D. S. & Tian, Z. Y., Graphical representation of the sub-solidus phase relationships in the reciprocal salt system Si, Al, Y/O, N. *Sci. China (Series A)*, **35** (1992) 877–88.